International Journal of Computing and Digital Systems
ISSN (2210-142X)
Int. J. Com. Dig. Sys. 15, No. 1 (Mar-24)

http://dx.doi.org/10.12785/ijcds/150180

IoMT-based Heart Rate Variability Analysis with Passive FBG Sensors for Improved Health Monitoring

Maitri Mohanty [1], Premansu Sekhara Rath [2] and Ambarish G. Mohapatra [3]

[1, 2]*Department of Computer Science and Engineering, GIET University, Gunupur Odisha, India*
[3]*Department of Electronics Engineering, Silicon University, Bhubaneswar, Odisha, India*

Received 29 Jul. 2023, Revised 7 Feb. 2024, Accepted 8 Feb. 2024, Published 1 Mar. 2024

Abstract: The use of smart healthcare systems to monitor cardiac parameters has gained widespread popularity globally due to advancements in technology. The Internet of Medical Things (IoMT) has become an integral part of modern healthcare by facilitating the efficient monitoring of vital signs through advanced sensors. Heart Rate variability (HRV) characteristics, which provide valuable insights into a patient's health, have become indispensable in healthcare applications. Fiber Bragg Grating (FBG) based optical sensors have emerged as cutting-edge technology for continuous monitoring of several cardiac parameters among the new alternatives. Recent technical advances have improved the accuracy of these sensors, allowing for the early identification and prognosis of heart illnesses, potentially saving lives. This article delves into the design, construction, and structural analysis of a passive optical FBG sensor capable of real-time acquisition of HRV parameters such as standard Deviation of Normal-to-Normal (SDNN), Root Mean Square of Successive Differences (RMSSD), and Percentage of Successive Normal-to-Normal intervals (PNN50) differing by more than 50 ms, along with Heart Rate (HR). It also provides enhanced signal processing methods as well as an IoT-based architectural architecture. Experimental research in a laboratory including five participants (three males and two females) revealed good performance, with an error rate of less than 10 percent when compared to a typical HR monitor. This intelligent technology detects arrhythmia, coronary heart disease, aortic disorders, and strokes with high accuracy, providing a substantial contribution to healthcare. The combination of Fiber Bragg Grating (FBG) sensors, Internet of Things (IoT) architecture, and cutting-edge technology has enormous potential for improving cardiac monitoring and patient outcomes.

Keywords: Fiber Bragg Grating sensor, IoMT, SDNN, RMSSD, PNN50, HR

1. Introduction

The Internet of Medical Things represents a burgeoning field in today's healthcare market, where a wide array of modern medical devices, software applications, and healthcare professionals converge on a unified platform to deliver high-quality services [1]. According to statistical analysis by the World Health Organization, various cardiac diseases account for 17.9 million deaths annually across the globe [2]. Among all countries, China, India, the US, and Canada have the highest rates of cardiovascular disease [3]. Therefore, Cardiovascular disease stands as a primary cause of increased mortality rates worldwide [3]. Heart rate variability serves as a valuable cardiac tool for assessing the autonomic nervous system [4]. Heart Rate Variability characterizes fluctuations of intervening time between successive heartbeats, reflecting the activity of the sympathetic as well as parasympathetic nervous systems [5]. Evaluating HRV parameters such as Standard Deviation of Normal-to-Normal intervals (SDNN), Root Mean Square of Successive Differences (RMSSD), Percentage of Successive NN intervals (PNN50) differing by more than 50 ms, and Heart Rate (HR) significantly contributes to diagnosing an individual's health condition [6,7]. So monitoring diverse cardiac parameters plays a vital role in detecting conditions such as cardiac arrest, asthma, dementia, pneumonia, and neonatal illnesses [8]. Consequently, continuous screening of these parameters provides medical practitioners with early detection capabilities, enabling them to save lives by identifying cardiac abnormalities at an earlier stage. Traditionally electronic devices are currently used to monitor vital parameters, and their utility is limited in certain scenarios, such as Magnetic Resonance Imaging (MRI) environments [9]. Furthermore, currently, patients are manually cared for within fixed time intervals by physicians and professional nurses in the Intensive Care Unit (ICU) [10]. Nevertheless, this approach is not suitable for people who need ongoing monitoring since they run the risk of consequences including diabetes, heart failure, or asthma attacks. So it is extremely difficult to continuously monitor cardiac parameters in the Intensive Care Unit (ICU).In the last decade, the development of optical sensors and advanced technologies has greatly accelerated the use of healthcare

E-mail address: maitri.mohanty@gmail.com, maitri.mohanty@giet.edu, premansusekhararath@giet.edu, ambarish.mohapatra@gmail.com

applications [11]. This newfound combination of medical equipment, passive sensors, software, and communication technologies has significantly improved the infrastructure of the healthcare business.

The advent of optical fiber sensors penetrates a paradigm shift, offering a new height to various domains such as communication, structural health monitoring, biomedicine, marine exploration, aerospace applications, and more [10,11]. Among the optical sensors available, Fiber Bragg Sensors (FBG) have emerged as an exceptional solution in the healthcare industry. Consequently, researchers have dedicated their efforts to developing FBG-based passive optical sensors for medical applications, both in noninvasive and invasive manners [11]. These sensors possess many advantageous aspects, including compact size, affordability, resistance to corrosive environments, chemical inertness, and robustness in high electrical and radio frequency settings [11, 12]. These sensors are flexible enough to measure an array of parameters, including strain, temperature, velocity pressure, acceleration, and tilt angle. [12].These sensors exhibit tremendous potential in providing effective solutions for challenging environments, including those with high radio frequency and electromagnetic interference. FBG passive sensor elements find applications in a multitude of smart healthcare setups, owing to their spectral encoding, multiplexing, and remote sensing capabilities [12, 13]. As a result, these sensors are embedded within various structures, further expanding the possibilities and advancements in the realm of smart healthcare applications. This work introduces a research initiative aiming to seamlessly integrate FBG sensors with IoMT for real-time healthcare monitoring. It emphasizes a comprehensive architectural framework, advanced signal processing, and contributions to scalable monitoring and decision support. The proposed distributed architecture aims to enable real-time monitoring of various heart rate variability parameters using the IoMT within distributed healthcare environments. The architecture comprises four layers: the sensing and data acquisition layer, the pre-processing of raw signals layer, the classification and diagnosis layer, and the visualization and analysis layer. In the sensing and data acquisition layer, which represents the intensive care unit (ICU) and a monitoring and control room, real-time data is acquired using FBG sensors. The FBG interrogator device, connected to a high-speed PC equipped with a Lab VIEW application, captures and analyzes the raw data before integrating it into the cloud application. The preprocessing layer handles the captured raw signal, which may be affected by unwanted noise, artifacts, and electromagnetic interference. The corrupted signal is filtered, and the peak of the signal is extracted using Fog computing technology. Local processing improves latency, enhances mobility, increases network bandwidth, aids in decision-making processes, and reduces traffic congestion issues. The classification and diagnosis layer involves forwarding the filtered data to the cloud computing environment for the estimation of heart rate variability parameters such as HR, SDNN, RMSSD, and PNN50, as well as body temperature, oxygen concentration, and environmental temperature. The processed data provides information about the patient's condition, detecting abnormalities based on predefined threshold values, and classifying patients as normal or abnormal. The data is stored in the cloud for future reference by healthcare professionals and researchers and serves as a backup in case of disaster conditions. In the visualization and analysis layer, the analyzed data results are sent to healthcare experts, nurses, and relatives. This real-time IoT-based cardiac monitoring system provides clinical reports to guide healthcare professionals, enabling them to take timely actions and prevent critical situations, ultimately saving lives.

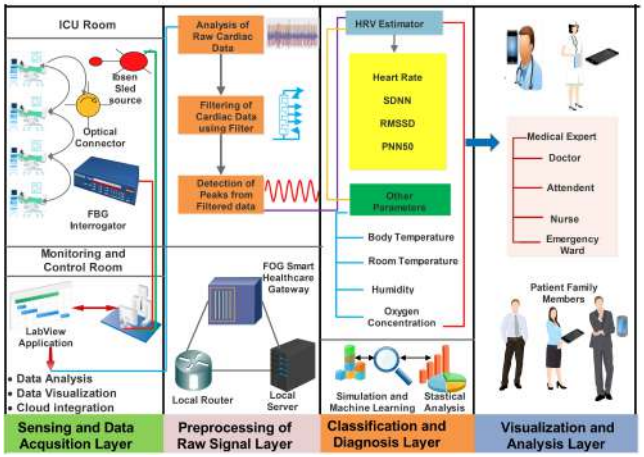

Figure 1. Architectural diagram of proposed IoT-based Cardiac monitoring System with FBG sensor

This article presents a real-time smart healthcare monitoring system, which is divided into eight sections for clarity. The initial section introduces the evolution of state-of-the-art technology, focusing on the optical Fiber Bragg Grating (FBG) sensor. This includes an exploration of its application areas and the advantages it offers in the realm of cardiac monitoring. Section 2 describes various related works, discussing them comprehensively and representing their results through a literature study. In Section 3, the fabrication, design, and working principle of FBG sensors are described. Section 4 outlines the description of the experimental setup employed for conducting laboratory experiments. This encompasses a mathematical design founded on the Finite Element Analysis (FEA) method, designed to simulate the manufacturing process of FBG sensors. Moving on to Section 5, the focus shifts to the objectives of real-time cardiac parameters monitoring within the context of a smart healthcare system. Furthermore, the Discussion and Observations are explained in section 6 which delves into the utilization of an advanced signal processing algorithm. This algorithm is applied to estimate various heart rate variability parameters, including HR, SDNN, RMSSD, and PNN50. The discussion places particular emphasis on presenting detailed insights into the corresponding results derived from this signal-processing approach. Section 7

encapsulates the conclusions drawn from the study. Lastly, the acknowledgment and reference section serves as a compilation of papers cited in this article, providing readers with additional resources for further exploration.

2. Literature Survey

Numerous articles have been published to explore the configuration, investigation, and application of FBG sensors in healthcare applications for monitoring vital sign parameters. These sensors have been employed to monitor various measurements such as Respiration Rate (RR), Heart Rate (HR), Oxygen concentration, environment temperature, and body temperature in both MRI and clinical settings. The dissemination of research findings in these articles contributes to the advancement of FBG sensor technology and its applications with cutting-edge technology in the healthcare sector.

In their 2023 work [14], Shi et al. introduce a compact, high-precision FBG sensor designed for real-time monitoring of cardiovascular pulse parameters, including HR, carotid augmentation index, left ventricular ejection time, and ejection duration index. The sensor boasts a sensitivity of 1547.3 pm/N and successfully converts longitudinal pulse input through a force-sensitive flexure.L. Zhichao et al. (2023) [15] present a portable home-based cardiopulmonary parameter detection system using Fiber Bragg Grating (FBG) and an adaptive K-value-based Variational Modal Decomposition (K-VMD) algorithm, demonstrating accurate results and better performance compared to traditional techniques for monitoring cardiopulmonary parameters in healthcare. F. De Tommasi et al. (2023)[16] explore the potential of Fiber Bragg grating (FBG) sensors in a 13-FBG array mattress for non-intrusive cardiorespiratory monitoring, showing promising accuracy in continuous heart rate estimation across diverse conditions. D. S. Ahmed et al. (2023) [17] published a human blood pressure sensor design that uses Fibre Bragg Grating (FBG) with a constant period of spacing. The sensor exhibits linearity, sensitivity, and observable changes in peak power and Bragg wavelength when pressure is applied. In a chest belt, C. Tavares et al. (2022) [18] weave a single FBG. The signal is filtered using a bandpass filter ranging from 0.8 Hz to 2 Hz to extract the HR and RR measurements. In (2022) [19], X. Wang et al. showcase the durability of Fiber Bragg Grating (FBG) sensors against vibration and bending, unveiling a body temperature tracking garment featuring waterproof and electromagnetic interference-resistant integrated FBG sensors, ensuring high resolution, rapid response, and applicability in scenarios like MRIs and ultrasounds. In their (2022) [20]study, M. Ladrova et al. investigate the application of Fibre Bragg Grating (FBG) sensors for cardiorespiratory monitoring during Magnetic Resonance Imaging (MRI), highlighting advantages such as electromagnetic interference resilience and reusability, while underscoring the need for further research due to challenges like signal delays and optimal sensor placement. To predict respiratory flow from wearable FBG sensors, M. Filosa et al. (2022) [21] introduce a meta-learning approach using LSTM neural networks. They indicate superior accuracy and establish the algorithm's potential for useful health applications.

A thorough examination of FBG sensors for tracking cardiac and respiratory parameters is presented in Table 1.

TABLE I. Methods for Vital Sign Parameters

Sl. no	Authors Details	Sensor technology	Using methods for parameter extraction	Limitation
1	Shi et al.(2023)[14].	FBG pulse probe.	Six-bar parallel mechanism for HR.	Inadequate IoMT-FBG discussion
2	L. Zhichao et al.(2023)[15].	FBG elastic strap.	K-VMD algorithm for HR and RR.	Fewer data on model generalization.
3	F. De Tommasi et al.(2023)[16].	FBG in mattress.	Signal filtering for RR, HR.	Lacks sample details.
4	C. Tavares et al. (2022) [18].	Single FBG Sensor.	Bandpass filter detects HR peaks.	Inadequate IoMT-FBG discussion
5	X. Wang et al.(2022)[19].	FBG in the garment.	Advanced Signal processing method for temperature.	Only track human body temperature.
6	M. Krej et al. (2021) [23].	Mat on flexible Plexiglass board.	TCN for HR detection.	Fewer data on model generalization.

In (2022) [22], A.A. Suryandi et al. explore cardiorespiratory monitoring during magnetic resonance imaging (MRI), emphasizing Fiber Bragg Grating (FBG) sensors with benefits such as electromagnetic interference resistance and reusability, while acknowledging challenges like signal delays and optimal sensor placement, underscoring the necessity for further research to develop a comprehensive monitoring system suitable for clinical applications. Moreover, M Krej et al. (2021) [23], a sensor mat consisting of nine arrays of Fiber Bragg Grating sensors has been proposed, with sensors arranged orthogonally within a

single-mode fiber. These sensors are mounted on a flexible Plexiglas board to capture Heart Rate (HR) readings from various sensor locations. The acquired BCG signal is preprocessed using decimation and bandpass filters. In (2021),[24] D. Ferraro et al. present an innovative Fibre Bragg Grating-based soft sensor for cardiac activity monitoring, showing promise in tests on isolated ovine (Ovis aries) hearts for real-time ventricular beat tracking with a remarkable tracking error of 2.7 ± 0.7 beats per minute. The sensor's consistent precision of less than 1 bpm is demonstrated in monitoring healthy adult minipig hearts, establishing its reliability. Similarly, Xin Cheg (2020) [25] introduces a deep-learning Temporal Convolution Network (TCN) for HR detection. A novel and efficient method is used for the fabrication of a Polymer Optical Fiber Bragg Grating (POFBG) sensor using a 25 nm - 248 nm UV laser radiation pulse solely on ZEONEX-based POFS. This sensor demonstrates the capability to differentiate between exhalation and inhalation during breath holds within the human respiration process. Also, Daniela Lo Presti et al. (2019) [26] demonstrate the fabrication of a Fiber Bragg Grating (FBG) within an elastic band to monitor Heart Rate and Respiration Rate. To calculate the heart rate during periods of quiet breathing and apnea, a customized algorithm along with a Butterworth filter is employed. Meanwhile, Shouhei Koyama and Hiroaki Ishizawa (2019) [27] describe that the FBG sensor is put near the wrist radial artery of a person. The captured signal undergoes filtering, and the Complete Ensemble Empirical Mode Decomposition with Adaptive Noise (CEEMDAN) technique is utilized to calculate both Heart Rate (HR) and Respiratory Rate (RR). At the same time the work presented by Ken Ogawa et al. (2019) [28] that a plethysmograph monitoring system is developed utilizing a fiber Bragg grating interrogator. Two FBGs are strategically positioned on the brachial artery. To measure Heart Rate (HR), a second-order Butterworth bandpass filter with a cutoff frequency ranging from 0.5 Hz to 5 Hz is employed. Similarly, Y. Haseda et al. (2019) [29] focus on, the FBG sensor is fabricated using both plastic optical fiber and silica optical fiber. The captured signal is subsequently filtered within the range of 0.5 Hz to 5 Hz. A partial least square regression method is applied to calculate blood pressure and pulse wave measurements. Interestingly, the pulse wave signal reveals that the FBG sensor fabricated with plastic optical fiber provides an eight-fold higher signal-to-noise ratio compared to the FBG sensor fabricated with silica optical fiber Moreover, in a study by M. Krej et al. (2019) [30], they designed an FBG sensor interrogator tailored for plethysmography, employing diverse machine learning techniques, among which random forest demonstrated superior performance. This approach yielded a Root Mean Square Error (RMSE) of 1.48 rpm for respiratory rate. In a similar vein, Ken Ogawa et al. (2018) [31] present a cloth-based setup featuring a single FBG sensor. This configuration enables the monitoring of respiration signals, PCG (Phonocardiogram), and ACG (Apex cardiogram) within the pericardium area of the heart. To detect the respiration rate, the captured data undergoes preprocessing using a second-order Butterworth filter with a low cutoff frequency of 0.2 Hz. PCG and ACG signals are recorded using a medium bandpass filter and a high-pass filter respectively. Additionally, J. Nedoma et al. (2018) [32] investigated setups utilizing biocompatible Polydimethyl-Siloxane (PDMS) along with FOI and FBG probes positioned on the chest. Bandpass filters were employed to determine respiratory rate (RR) and heart rate (HR). The obtained results demonstrate satisfactory performance when compared to the reference device. Ibrahim Sadek et al. (2015) [33] propose a setup consisting of a mat with four sensor arrays for acquiring the Ballistocardiogram (BCG) signal from the human body. The acquired signal is subsequently filtered, and the Complete Ensemble Empirical Mode Decomposition with Adaptive Noise (CEEMDAN) method is employed to calculate the heart rate. In addition, Y. Zhu et al. (2014) [34] have introduced an arrangement of Fiber Bragg Gratings (FBGs) positioned on a mat. The signals captured by various sensors within the same array are fused using cepstrum analysis. To detect heart rate (HR) from the chest area, a bandpass filter with a cutoff frequency ranging from 0.5 Hz to 20 Hz is employed. In their study, L. Dziuda et al. (2013) [35] demonstrate the placement of an FBG sensor inside a bed mattress. The Ballistocardiogram (BCG) signal is filtered using a bandpass filter with a frequency range of 2 Hz to 60 Hz to extract respiratory rate (RR) and heart rate (HR) measurements. The maximum relative error for RR is reported as 7.67Additionally, the location of an FBG sensor on the human body is described by Y. Miyachi et al. (2013) [36] for both the neck and ankle regions. Using a lowpass filter with a cutoff frequency of 5 Hz, the collected signal is filtered. A first derivative procedure is used to find peaks to quantify heart rate and respiration rate correctly. When compared to a reference device, namely a sphygmomanometer, the findings reveal a 5 percent inaccuracy.

While certain studies acknowledge challenges such as signal delays and optimal sensor placement, there is a shortfall in thoroughly examining potential limitations and practical obstacles in implementing Fiber Bragg Grating (FBG) sensors. Insufficient details on methodologies and the absence of standardized protocols affect result comparability. This research aims to integrate FBG sensors with IoMT for real-time healthcare monitoring, proposing a four-layered framework. The focus is on implementing advanced signal processing for estimating critical health indicators.

3. Operational Principle of Optical Sensors Based on Fiber Bragg Grating

FBG sensors have revolutionized healthcare applications due to their compact size, affordability, lightweight nature, resistance to harsh environments, and absence of temperature drift [37]. These sensors operate based on the principle of high-reflection light phenomena. The grating region of an FBG is created through various established techniques like the phase mask technique, interferometer technology, and femtosecond pulsed laser technique, by incidenting UV

light to the optical fiber core [38, 39]. This process generates a persistent periodic change in the refractive index of the optical fiber core, resulting in a reflective selective filter. When high-intensity light goes through the optical fiber in the longitudinal direction, a narrow bandwidth-centered wavelength is reflected, satisfying the Bragg condition and known as Bragg wavelength. Variations in the fiber core's effective refractive index and grating pitch's periodicity are correlated with the alternation of Bragg wavelength. Figure 2 illustrates the operational fundamentals of an FBG sensor, which relies on the light reflection phenomena. As mentioned by coupled-mode theory, peak Bragg wavelength is determined by [40] in Equation 1

$$\ddot{\lambda_b} = 2n_{eff}\Lambda \tag{1}$$

Where, n_{eff} is the modified optical fiber core's effective refractive index. Λ is the periodicity of the pitch. Equation 1 can be alternatively expressed as Equation 2

$$\frac{\delta\ddot{\lambda}_b}{\lambda_b} = \left(\frac{1}{\Lambda}\frac{\delta\Lambda}{\delta\varepsilon} + \frac{1}{\eta_{eff}}\frac{\delta\eta_{eff}}{\delta\varepsilon}\right)\Delta\varepsilon + \left(\frac{1}{\Delta}\frac{\delta\Lambda}{\delta T} + \frac{1}{\eta_{eff}}\frac{\delta\eta_{eff}}{\delta T}\right)\Delta T \tag{2}$$

The variation in peak Bragg wavelength with respect to applied strain with temperature zero is represented in Equation 3

$$\frac{\delta\ddot{\eta}_{eff}}{\eta_{eff}} = \eta_{eff}^2\left[P_{12} - \nu\left(P_{11} - P_{12}\right)\right] \tag{3}$$

Equation 3 can be equivalently expressed as Equation 4.

$$\ddot{P}_e = \frac{\eta_{eff}^2}{2}\left[P_{12} - \nu\left(P_{11} + P_{12}\right)\right] \tag{4}$$

Where, P_e Represents the coefficient of optical strain in a fiber. P_{ij} are the strain optical components of a tensor. ν is Poisson's ratio.

From (3) and (4), the variation of peak Bragg wavelength is represented in Equation 5

$$\ddot{\Delta}\lambda_b = \left(1 - P_e\right)\lambda_b\varepsilon \tag{5}$$

The variation in peak Bragg wavelength with applied temperature and zero strain is given by Equation (6)

$$\ddot{\Delta}\lambda_b = \lambda_b\left(\frac{1}{\eta_{eff}}\frac{\delta\eta_{eff}}{\delta T} + \frac{1}{\Lambda}\frac{\delta\Lambda}{\delta T}\right)\Delta T \tag{6}$$

Equation (6) can alternatively be expressed as Equation (7)

$$\ddot{\lambda}_b\left(\alpha + \beta\right)\Delta T = K_T\lambda_b\Delta T \tag{7}$$

The value of α, β, γ are represented in Equation (8),Equation (9),Equation (10)

$$\ddot{\alpha} = \frac{1}{\Lambda}\frac{\delta\Lambda}{\delta T} \tag{8}$$

$$\ddot{\beta} = \frac{1}{\eta_{eff}}\frac{\delta\eta_{eff}}{\delta T} \tag{9}$$

$$_T = \alpha + \beta \tag{10}$$

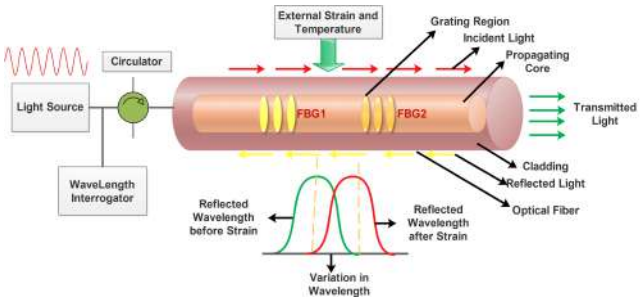

Figure 2. The operational principle of an FBG sensor

Following the selection of the material for the grating zone, the material's strain sensitivity coefficient and temperature sensitivity coefficient are applied for sensor sensing.

4. Experimental Set-up

In the phase mask technique, a periodic interference pattern is generated by exposing the optical fiber core to high-intensity ultraviolet light. The resulting grating region serves as the sensing region for measuring parameters such as strain and temperature. In the controlled laboratory environment, the experiments were carried out using an industrial polymer material known as polydimethylsiloxane (PDMS) to craft the sensor component. Figure 3 depicts the fabricated FBG sensor, which is coated with a sandwiched structure of polydimethylsiloxane to enhance sensitivity by four times compared to a bare FBG. This sensor is positioned within a chest belt to capture real-time cardiac signals through the chest wall's movement. For structural analysis of the sensor elements, a Finite Element Analysis (FEA) method is employed using COMSOL Multiphysics software. The FBG optical sensor is incorporated into PDMS material, forming the sensor unit.

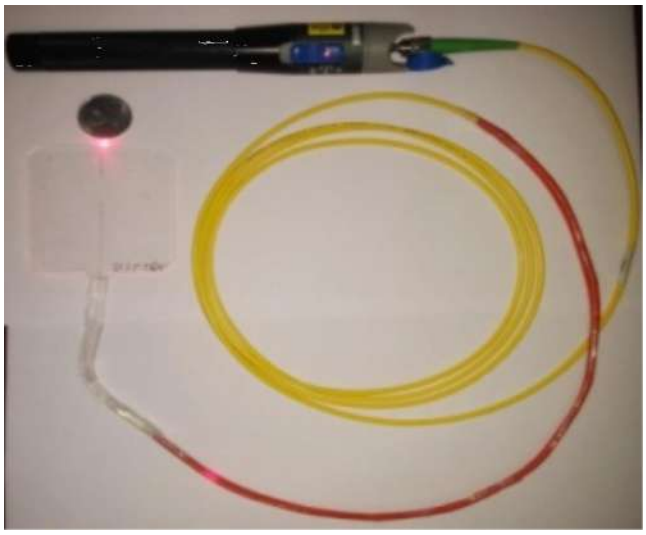

Figure 3. Fabricated FBG Sensor

To connect with the FBG sensing component, an Ibsen IMON 512 High-speed FBG interrogator and a high-intensity light source (Ibsen SLED) with a central wavelength of 1550 nm (Ibsen DL-BP1-1501A SLED) are utilized. A dedicated PC with specific specifications, including a 6th generation Intel Core i5 processor, 8 GB RAM, and a 512 GB internal Solid-State Drive, enables swift acquisition of the cardiac waveform through the FBG sensor. The interrogator unit of FBG and the PC are linked through a high-speed Gigabit switch serving as the LAN interface. Data collection is coordinated using the LabVIEW platform, and a vendor-supplied proprietary DLL library file is utilized to construct the acquisition application. The detailed laboratory setup is illustrated in Figure 4.

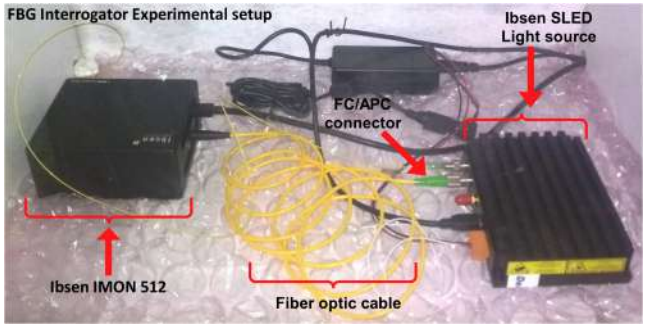

Figure 4. Experimental set-up

Table 2 and Table 3 illustrate the dimensions of the fabricated FBG element and the configuration used for simulation.

TABLE II. Dimension of the 3D sensor model

Parameters	Dimension
Effective Length	40 mm
Effective Width	40 mm
Effective Thickness	2 mm

TABLE III. Configurations for Simulation

Simulation Configuration	Parameters
Material	polydimethylsiloxane
Applied Frequency	0.33 Hz
Acts per minute	20 acts per minute

5. Real-Time Cardiac Parameters Monitoring Objectives

The key sensing component in this monitoring system consists of a tailor-made FBG sensor manufactured on a single fiber optics cable. FBGs can be incorporated into a substrate composed of a composite polymer material such as PDMS to enhance sensitivity compared to using bare FBGs. Conventional electrical devices have difficulties in high electromagnetic environment settings, like MRIs, where patient skin may be damaged and image quality may be compromised. The current healthcare system is unable to meet the needs of patients in Intensive Care Units (ICUs), who require round-the-clock care and real-time monitoring. The fusion of FBG sensors with IoT systems for monitoring Cardiac Variability metrics signifies a notable advancement in healthcare technology. This proposed study is to introduce an affordable cardiac monitoring application that can be used with current MRI machines and intensive care units, hence facilitating future research and development. Figure 5 displays the representational diagram of the process of cardiac measurement. The proposed cardiac measurement process consists of the following sub-elements such as denoising, peak detection model, estimation model for SDNN, pNN50, RMSSD, and HR, etc.

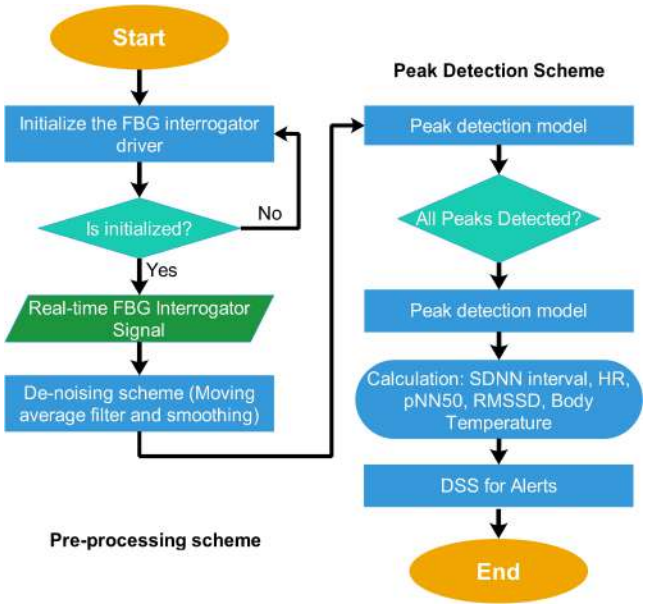

Figure 5. Flow diagram of the proposed cardiac measurement Scheme

Also, the planned work satisfies a wide industrial need in the healthcare industry. The novel optical sensing technology will enable medical practitioners to evaluate heart variability measures in the ICU and during MRI testing, broadening its industrial applicability beyond present circumstances.

6. Discussion And Observations

Under controlled environmental conditions, an experimental procedure included five participants aged between 30 and 40. These participants were classified into two categories: normal and abnormal. Four of them were normal subjects, while one had arrhythmia. Real-time cardiac signals were collected from all participants using an FBG sensor within a laboratory setting. The given Table 4 presents information on the Experimental Configuration Setup.

The acquisition signal's sampling frequency is 1000 Hz. The obtained BCG signals are vulnerable to various artifacts, including disturbances from motion, environmental noise, and coupling effects. So, the BCG raw signal undergoes analysis using Fast Fourier Transformation, re-

TABLE IV. Experimental Configuration Setup

Experimental Configuration	Type
High-intensity SLED source	Ibsen SLED
Interrogator unit	Ibsen IMON 512
High-speed PC	Intel Core i5 six generations, 8 GB RAM
Software for Simulation	COMSOL Multiphysics software, MATLAB software

vealing interference and noise above 10 Hz. To mitigate the corrupted cardiac signal in real-time, a bandpass IIR filter is designed using MATLAB, with a range of 10 Hz to 140 Hz. Table 5 shows the configuration of the designed filter to nullify the corrupted signal.

TABLE V. Parameters for the design of a filter

Filter Type	IIR bandpass Filter
PassBand Frequency	10 Hz
StopBand Frequency	140 Hz
Sampling Frequency	1000Hz
PassBand Ripple	1dB
Stopband Attenuation	1.5dB

Also in signal filtering, particularly for complex signals, comprehending group delay characteristics is crucial. Group delay, intricately linked to a filter's phase response, measures the time delay for various frequency components as they traverse the filter. In a similar context, post-filtering, a

TABLE VI. HRV Parameters for Normal Person

Parameters	Age Range	Heart Condition	Parameters Range
Mean HR [40]	30-40	Normal	Min=55bpm Max=105bpm
SDNN [41]	30-40	Normal	Min=20.4ms Max=51.4ms
RMSDD[40]	30-40	Normal	Min=11.7ms Max=42.9ms
pNN50 count [40,41] [40]	30-40	Normal	Min=3 percentage Max=23 percentage

peak detection algorithm is designed to locate signal peaks within a 10-second timeframe. This algorithm accurately identifies peaks corresponding to individual heartbeats in the output of the FBG sensor, falling within the wavelength range of 1545.7 nm to 1545.9 nm. These identified peaks play a vital role in evaluating HRV parameters, including Standard Deviation of Normal-to-Normal intervals (SDNN), pNN50 (percentage of successive NN intervals differing by more than 50 ms), Root Mean Square of Successive Differences (RMSSD), and Heart Rate (HR).HRV serves as a crucial diagnostic indicator for diseases [33], with research suggesting that higher HRV values indicate increased stress resilience and lower mortality rates. Table 6 presents information on various HRV parameters such as HR, SDNN, pNN50, and RMSSD for a normal individual.To depict the results, Figures 6 through 10 present the raw Ballistocardiogram (BCG) cardiac signals acquired from four individuals with normal cardiac function and one individual with arrhythmia. Additionally, Figures 11 through 15 showcase the spectrograms of these five subjects. Furthermore, Figures 16 through 20 depict the filtered signals, distinguishing between four individuals with normal cardiac function and one individual with an abnormal cardiac condition.

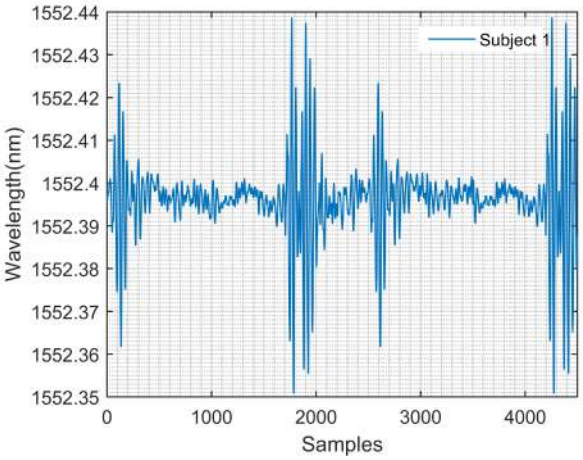

Figure 6. Raw Signal of Normal Subject 1

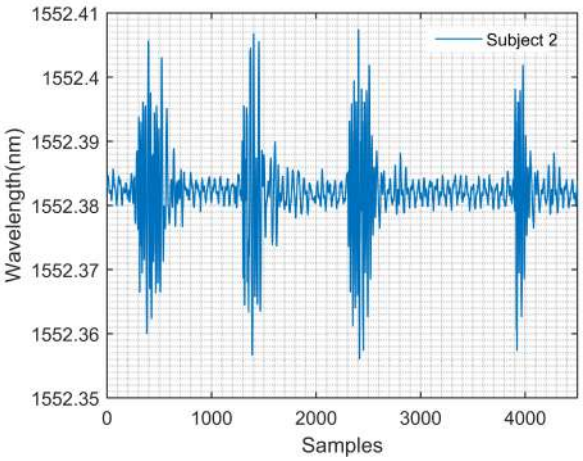

Figure 7. Raw Signal of Normal Subject 2

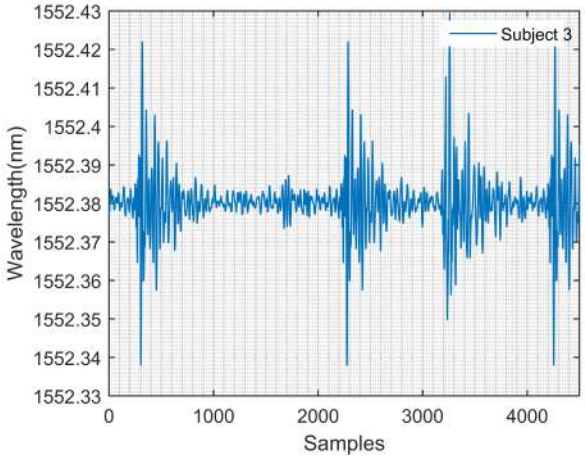

Figure 8. Raw Signal of Normal Subject 3

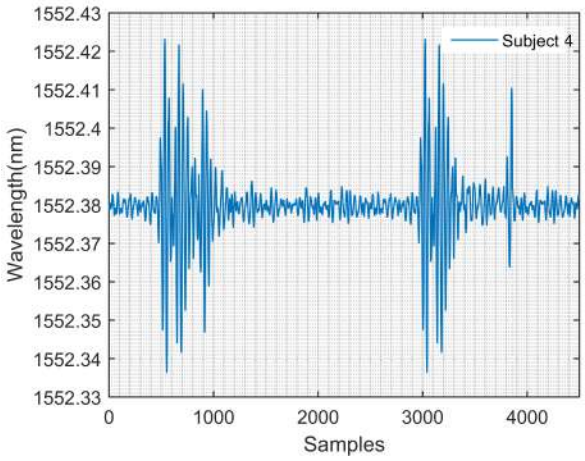

Figure 9. Raw Signal of Normal Subject 4

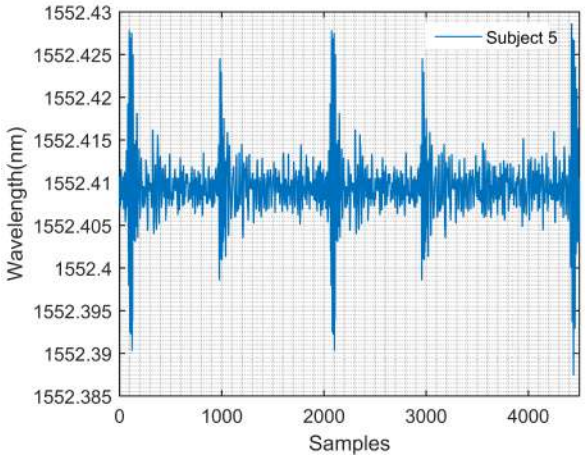

Figure 10. Raw signal of Arrhythmia Subject 5

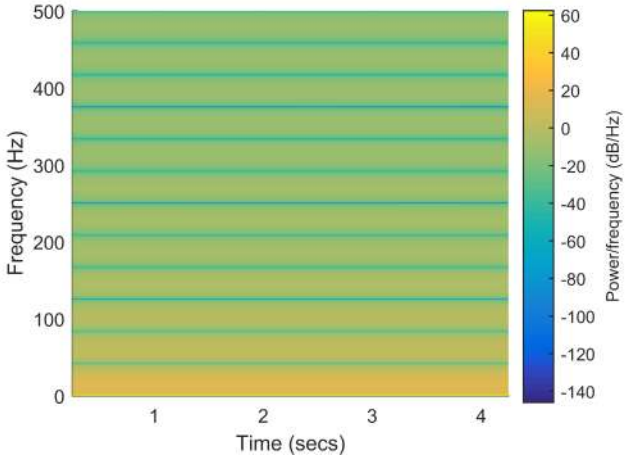

Figure 11. Spectrogram of Normal Subject 1

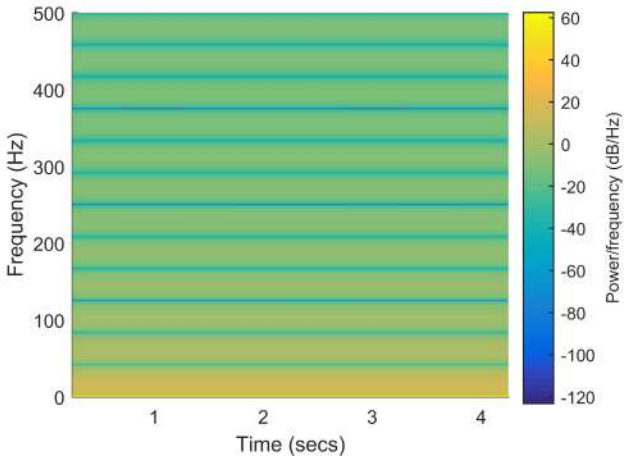

Figure 12. Spectrogram of Normal Subject 2

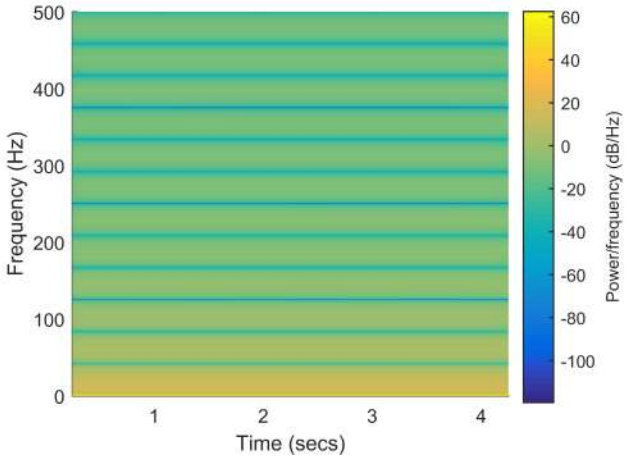

Figure 13. Spectrogram of Normal Subject 3

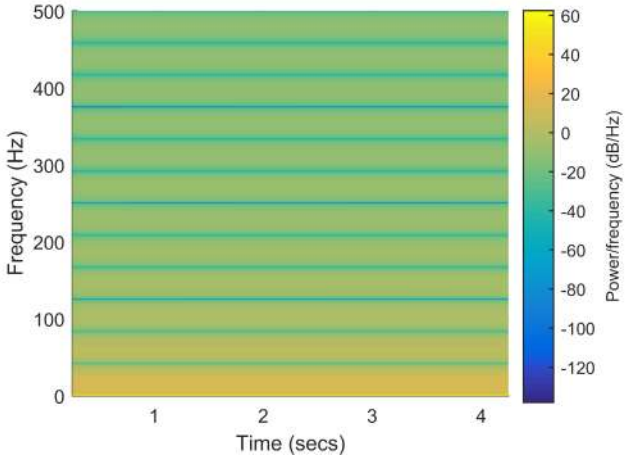

Figure 14. Spectrogram of Normal Subject 4

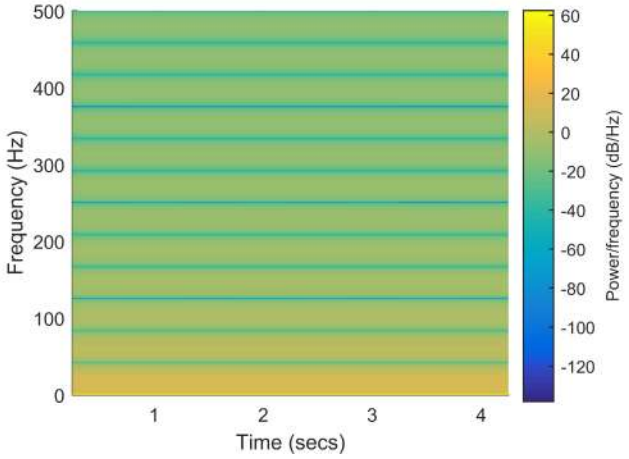

Figure 15. Spectrogram of Arrhythmia Subject 5

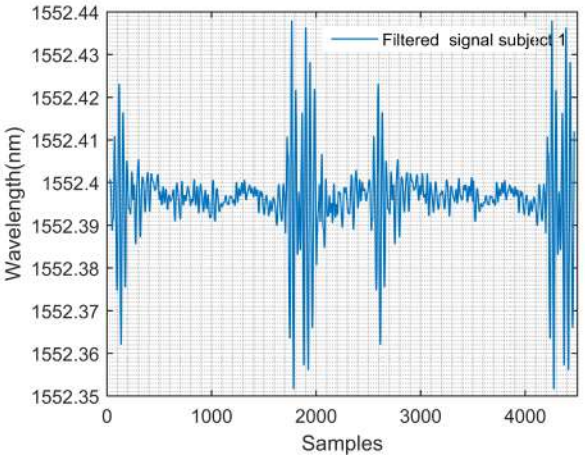

Figure 16. Filtered Signal of Normal Subject 1

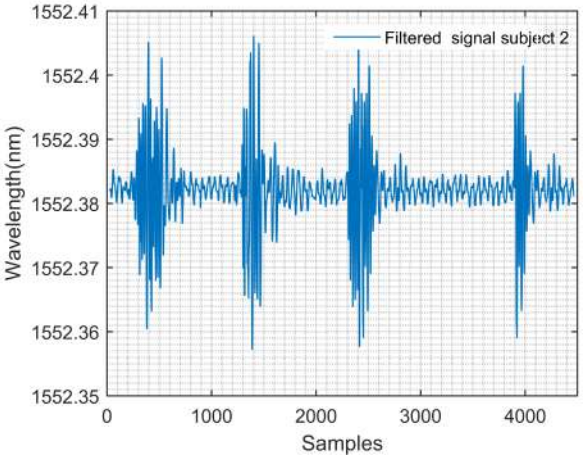

Figure 17. Filtered Signal of Normal Subject 2

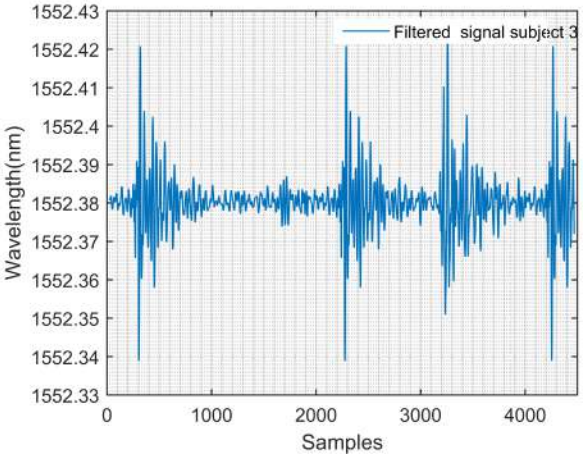

Figure 18. Filtered Signal of Normal Subject 3

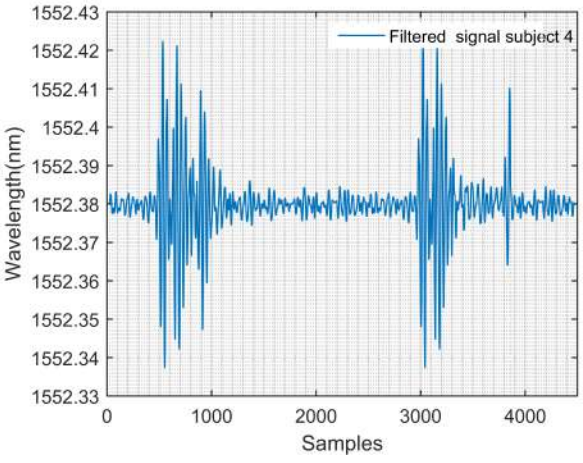

Figure 19. Filtered Signal of Normal Subject 4

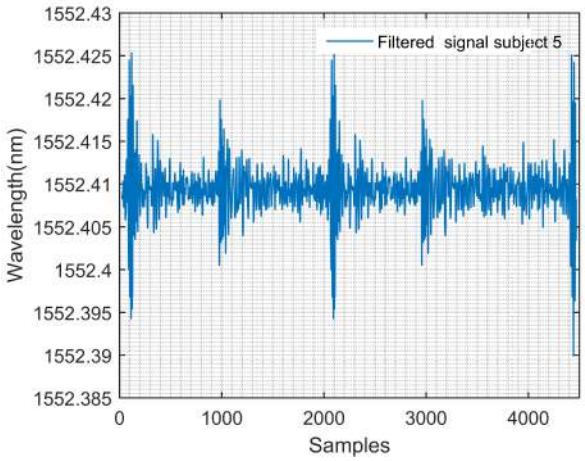

Figure 20. Filtered Signal of Arrhythmia Subject 5

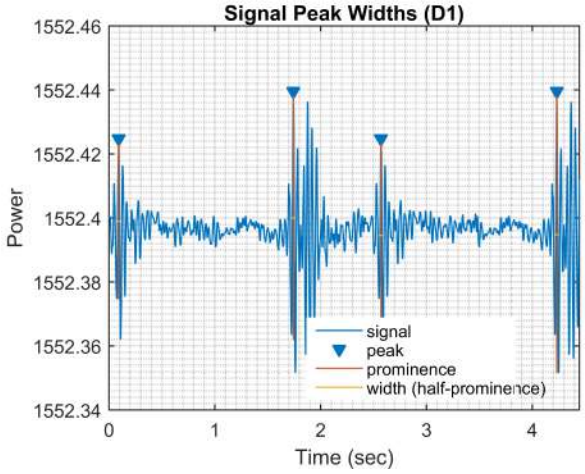

Figure 21. Peak Detection of Normal Subject 1

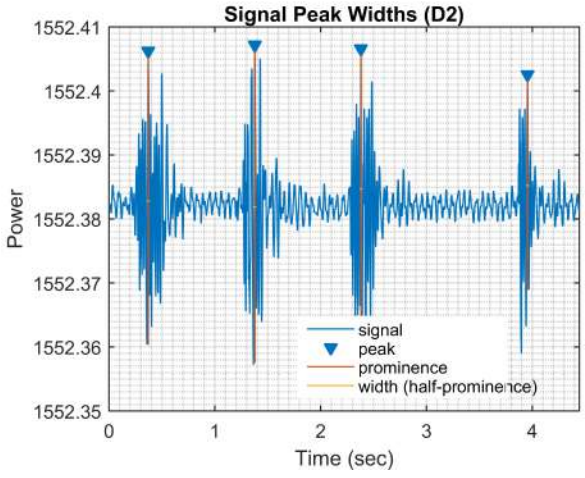

Figure 22. Peak Detection of Normal Subject 2

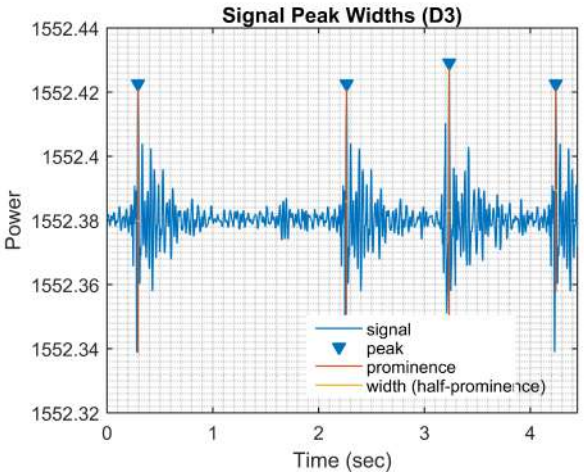

Figure 23. Peak Detection of Normal Subject 3

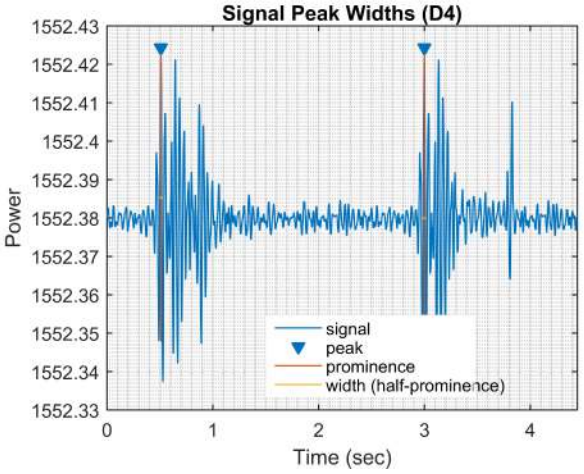

Figure 24. Peak Detection of Normal Subject 4

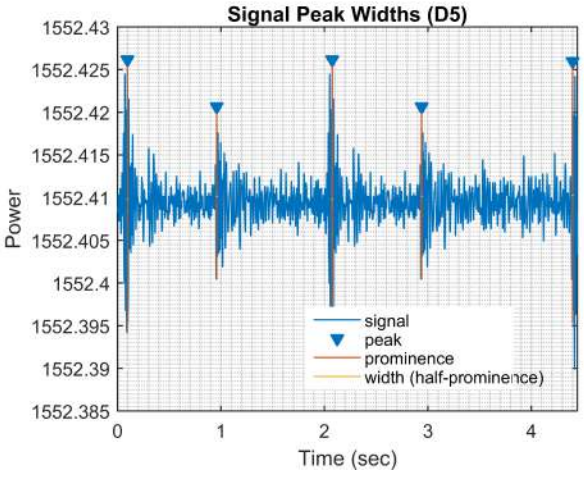

Figure 25. Peak Detection of Arrhythmia Subject 5

Table 7 displays the Heart Rate Variability Parameters recorded by an FBG sensor for various subjects participat-

ing in the experiment.

TABLE VII. Different Heart rate variability Parameters of subjects involved in the experiment

Subject	Mean Heart Rate (HR)	The standard deviation of NN intervals (SDNN)	Root mean Square of Successive differences (RMSSD	pNN50
1	58.4300	28.2827 ms	24.4014 ms	9.000 percentage
2	68.2948	33.4786 ms	25.8290 ms	7.000 percentage
3	60.5076	37.3285 ms	22.4038 ms	12.000 percentage
4	70.5712	35.5661 ms	30.7069 ms	15.000 percentage
5	50.0964	20 ms	10.02 ms	2 percentage

Table 8. Validation of HRV parameters using Standard HRV monitor for subject 3

TABLE VIII. Validation of HRV parameters using Standard HRV monitor

HRV parameters in the Supine position	Using FBG sensor	Standard HRV monitor	Error in percentage
Mean HR	60.5076	65.50	7.63 percentage
SDNN	37.3285 ms	36.3106 ms	2.7 percentage
RMSDD	22.4038 ms	23.4101 ms	4.31 percentage
pNN50 count	12.00 percentage	12.25 percentage	2.04 percentage

The outcomes of the proposed system are outlined in Table 7, while Table 8 displays the results obtained from a standard Heart Rate Variability (HRV) monitor, serving as a reference device. The HRV parameters of the normal and abnormal subjects involved in the experiment are calculated while in the supine position. The findings reveal that the proposed sensor produces satisfactory results, with an error of less than 10 percent compared to the reference device. Other performance matrices' Sensitivity and Specificity also gave the same values for both ensembles. Thus, both are considered for the best results.

7. Conclusions And Future Work

The Finite Element Analysis is instrumental in formulating and designing the Fiber Bragg Grating (FBG) element, incorporating a comprehensive structural analysis of the sensor element. Enhancing the FBG sensor's sensitivity involves the application of polydimethylsiloxane (PDMS). In a laboratory setting, real-time environment cardiac signals are obtained by the FBG sensor, and a bandpass Infinite Impulse Response (IIR) filter is developed for pre-processing the raw signals. Employing advanced signal processing algorithms allows the extraction of various Heart Rate Variability (HRV) parameters, including SDNN intervals, RMSDD, HR, and pNN50. Experimental results indicate an error rate of less than 10 percent compared to the reference device, showcasing the commendable performance of the proposed FBG sensor. This achievement not only underscores the potential integration of the FBG sensor in the healthcare domain but also paves the way for remote observation and foremost disease diagnosis through IoMT. The experiment focuses on a specific age group of participants placed in a supine position. The durability and long-term dependability of Fibre Bragg Grating (FBG) sensors for continuous cardiac monitoring have yet to be well studied, raising concerns about their sustained performance over extended periods. In future endeavors, focus on advancing signal processing algorithms to achieve heightened accuracy in extracting essential cardiac parameters from FBG sensor data. Undertake thorough and extended reliability investigations to assess the enduring performance of FBG sensors for continuous cardiac monitoring, and aim to establish standardized procedures to ensure consistency and comparability across diverse research projects and medical applications.

Here are the references: [1], [2], [3], [4], [5], [6], [7], [8], [9], [10], [11], [12], [13], [14],[15],[16],[17],[18],[19],[20],[21],[22],[23],[24], [25], [26], [27], [28], [29], [30], [31], [32], [33], [34], [35], [36], citeWerneck2013, [37], [38], [39], [40]

8. Acknowledgement

The authors wish to convey their thanks to the Silicon Institute of Technology, Bhubaneswar, and the Central Glass and Ceramic Research Institute (CGCRI), Kolkata, for their consistent support in crafting the FBG sensor during the research. Additionally, the authors express gratitude to the Silicon Institute of Technology, Bhubaneswar, for supplying crucial licensed software such as LabVIEW and FBG interrogator. These tools played a crucial role in the effective implementation of the experiment.

References

[1] A. C. L. V. A. Zanella, N. Bui and M. Zorzi, "Internet of things for smart cities," *IEEE Internet of Things Journal*, pp. 22–32, 2014.

[2] U. M. Jadhav, "Cardio-metabolic disease in india—the up-coming tsunami," *Annals of Translational Medicine*, vol. 6, 2018.

[3] L. H. W. C. H. K. S. C. Deaton, E. S. Froelicher and T. Jaarsma, "The global burden of cardiovascular disease," *European Journal of Cardiovascular Nursing*, vol. 10, pp. S5–S13, 2011.

[4] L. K. McCorry, "Physiology of the autonomic nervous system," *American Journal of Pharmaceutical Education*, vol. 71, 2007.

[5] I. T. B. M. M. P. E. M. Ezzati, Z. Obermeyer and D. A. Leon, "Contributions of risk factors and medical care to cardiovascular mortality trends,," *Nature Reviews Cardiology*, vol. 12, pp. 508–530, 2015.

[6] F. Shaffer and J. P. Ginsberg, "An overview of heart rate variability metrics and norms," *Frontiers in Public Health*, vol. 12, 2017.

[7] S. K. T. D. H. M. R. Mehra, S. S. Desai and A. N. Patel, "Cardiovascular disease, drug therapy, and mortality in covid-19," *New England Journal of Medicine*, vol. 382, 2020.

[8] G. M. G. C. V. M. G. M. F. Sessa, V. Anna, "Heart rate variability as a predictive factor for sudden cardiac death," *Aging (Albany NY)*, vol. 10, p. 166, 2018.

[9] S. Umesh and S. Asokan, "A brief overview of the recent biomedical applications of fiber bragg grating sensors," *ournal of the Indian Institute of Science*, vol. 94, pp. 319–328, 2014.

[10] D. L. P. A. N. D. T. C. Massaroni, M. Zaltieri and E. Schena, "Fiber bragg grating sensors for cardiorespiratory monitoring: A review," *IEEE Sensors Journal*, vol. 21, pp. 14 069–14 080, 2020.

[11] N. G. J. Sahota and D. Dhawan, "Fiber bragg grating sensors for monitoring of physical parameters: A comprehensive review," *Optical Engineering*, vol. 59, pp. 060 901–060 901, 2020.

[12] P. B. L. C. S. Patel, H. Park and M. Rodgers, "A review of wearable sensors and systems with application in rehabilitation," *Journal of NeuroEngineering and Rehabilitation*, vol. 9, pp. 1–17, 2012.

[13] K. V. R. Rohan and P. Ranjan, "Recent advancements of fiber bragg grating sensors in biomedical application: a review," *Journal of Optics*, pp. 1–12, 2023.

[14] X. N. C. Shi, H. Zhang and K. Wang, "An fbg-based sensor with both wearable and handheld forms for carotid arterial pulse waveform measurement," *IEEE Transactions on Instrumentation and Measurement*, 2023.

[15] S. T. L. Zhichao, Z. Xi and M. Jiahe, "Heartbeat and respiration monitoring based on fbg sensor network," *Optical Fiber Technology*, vol. 81, p. 103561, 2023.

[16] M. A. C. M. C. E. S. F. De Tommasi, C. Massaroni and D. L. Presti, "Fbg-based mattress for heart rate monitoring in different breathing conditions," *IEEE Sensors Journal*, 2023.

[17] A. H. A. D. S. Ahmed and S. A. Kadhim, "Design and implementation of a human blood pressure monitoring system using an fbg sensor," vol. 2977, 2023.

[18] D. L. P. M. F. D. N. A. H. S. C. Tavares, C. Leitão and P. Antunes, "Respiratory and heart rate monitoring using an fbg 3d-printed wearable system," *Biomedical Optics Express*, vol. 13, pp. 2299–2311, 2022.

[19] J. Y. X. S. L. H. . L. X. Wang, X., "Fiber bragg grating-based smart garment for monitoring human body temperature," *Sensors*, vol. 11, p. 4252, 2022.

[20] N. J. M. R. B. K. . K. R. Ladrova, M., "Fiber-optic cardiorespiratory monitoring and triggering in magnetic resonance imaging," *IEEE Transactions on Instrumentation and Measurement*, vol. 71, pp. 1–14, 2022.

[21] M. L. F. D. D. G. D. J. A. A. . . O. C. M. Filosa, M., "A meta-learning algorithm for respiratory flow prediction from fbg-based wearables in unrestrained conditions," *Artificial Intelligence in Medicine*, vol. 130, p. 102328, 2022.

[22] S. N. M. A. P. V. . D. S. Suryandi, A. A., "Fiber optic fiber bragg grating sensing for monitoring and testing of electric machinery: Current state of the art and outlook," *Machines*, vol. 10, p. 1103, 2022.

[23] A. A. S. S. K. A. K. M. e. a. M. Krej, T. Osuch, "Deep learning-based method for the continuous detection of heart rate in signals from a multi-fiber bragg grating sensor compatible with magnetic resonance imaging," *Biomedical Optics Express*, vol. 12, pp. 7790–7806, 2021.

[24] D. G. C. D. Z. C. C. L. H. M. . . O. C. M. Ferraro, D., "Implantable fiber bragg grating sensor for continuous heart activity monitoring: ex-vivo and in-vivo validation," *IEEE Sensors Journal*, vol. 21, pp. 14 051–14 059, 2021.

[25] C. F. J. P. J. B. X. Cheng, D. S. Gunawardena and H. Y. Tam, "Single nanosecond-pulse production of polymeric fiber bragg gratings for biomedical applications," *Optics Express*, vol. 28, pp. 33 573–33 583, 2020.

[26] J. D. L. M. M. C. U. G. L. e. a. D. L. Presti, C. Massaroni, "Wearable system based on flexible fbg for respiratory and cardiac monitoring," *IEEE Sensors Journal*, vol. 19, pp. 7391–7398, 2019.

[27] H. I. S. Koyama and S. K. Liaw, "Vital sign measurement using fbg sensor for new wearable sensor development," *n Fiber Optic Sensing-Principle, Measurement and Applications, IntechOpen*, pp. 1–16, 2019.

[28] Y. H. K. F. H. I. K. Ogawa, S. Koyama and K. Fujimoto, "Wireless, portable fiber bragg grating interrogation system employing optical edge filter," *Sensors*, vol. 19, p. 3222, 2019.

[29] H. Y. T. S. C. S. K. Y. Haseda, J. Bonefacino and H. Ishizawa, "Measurement of pulse wave signals and blood pressure by a plastic optical fiber fbg sensor," *Sensors*, vol. 19, p. 5088, 2019.

[30] P. B. M. Krej and Dziuda, "Detection of respiratory rate using a classifier of waves in the signal from an fbg- based vital signs sensor," *Computer Methods and Programs in Biomedicine*, vol. 177, pp. 31–38, 2019.

[31] H. I. S. F. K. Ogawa, S. Koyama and K. Fujimoto, "Simultaneous measurement of heart sound, pulse wave, and respiration with single fiber bragg grating sensor," *In 2018 IEEE International Symposium on Medical Measurements and Applications (MeMeA)*, pp. 1–5, 2018.

[32] M. F. J. C. P. S. R. M. J. Nedoma, S.Kepak and P. Krupa, "Magnetic resonance imaging compatible non-invasive fiber-optic sensors based on the bragg gratings and interferometers in the application of monitoring heart and respiration rate of the human body: A comparative study," *Sensors*, vol. 18, p. 3713, 2018.

[33] V. F. S. F. I. Sadek, J. Biswas and M. Mokhtari, "Automatic heart rate detection from fbg sensors using sensor fusion and enhanced empirical mode decomposition," *In 2015 IEEE International Symposium on Signal Processing and Information Technology (ISSPIT)*, pp. 349–353, 2015.

[34] E. H. J. J. M. C. G. H. Z. e. a. Y. Zhu, V. F. S. Fook, "Heart rate estimation from fbg sensors using cepstrum analysis and sensor fusion," *In 2014 36th Annual International Conference of the IEEE Engineering in Medicine and Biology Society*, pp. 5365–5368, 2014.

[35] M. K. L. Dziuda and F. W. Skibniewski, "Fiber bragg grating strain sensor incorporated to monitor patient vital signs during mri," *IEEE Sensors Journal*, vol. 13, pp. 4986–4991, 2013.

[36] S. K. Y. Miyauchi and H. Ishizawa, "A basic experiment of blood-pressure measurement which uses fbg sensors," *In 2013 IEEE International Instrumentation and Measurement Technology Conference (I2MTC)*, pp. 1767–1770, 2013.

[37] D. A. J. L. Z. Y. J. Rao, D. J. Webb and I. Bennion, "Optical in-fiber bragg grating sensor systems for medical applications," *Journal of Biomedical Optics*, vol. 3, pp. 38–44, 1998.

[38] B. L. J. Chen and H. Zhang, "Review of fiber bragg grating sensor technology," *Frontiers of Optoelectronics in China*, vol. 4, pp. 204–212, 2011.

[39] C. B. D. P. W. J. F. T. H. O. G. M. N. Jarczok, K. Weimer and E. M. Balint, "Heart rate variability in the prediction of mortality: A systematic review and meta-analysis of healthy and patient populations," *Neuroscience Biobehavioral Reviews*, vol. 143, p. 104907, 2022.

[40] M. E. M. T. Vybiral, R. J. Bryg and W. E. Boden, "Effect of passive tilt on sympathetic and parasympathetic components of heart rate variability in normal subjects," *The American Journal of Cardiology*, vol. 63, pp. 1117–1120, 1989.

Maitri Mohanty is a Ph.D. research scholar in the Department of Computer Science and Engineering at GIET University, Gunupur, Odisha, India. She has completed her M.Tech and B.E from BPUT University, BBSR, Odisha, India. Her area of interest includes Fiber Bragg Grating sensors, machine learning, and the Internet of things.

Premansu Sekhara Rath is working as an Associate Professor in the department of Computer Science and Engineering at GIET University, Gunupur, Odisha, India. His current research interests include Network Security, AI, ML, Image processing, machine learning, Optical sensors, Internet of Things. He has published several journal and conference papers.

Ambarish G. Mohapatra is working as an Associate Professor in the Department of Electronic and Instrumentation Engineering at Silicon University, Bhubaneswar, Odisha, India. His current research interests include Optical sensors, Wireless Sensor networks, AI, machine learning Internet of Things. He has published several journal and conference papers.